CHINESE OPTICS LETTERS

Vol. 19, No. 4 | April 2021

Quantum wells micro-ring resonator laser emitting at 1746 nm for gas sensing

Fangyuan Meng (孟芳媛)[1,2,3], Hongyan Yu (于红艳)[1,2,3*], Xuliang Zhou (周旭亮)[1,2,3**], Yajie Li (李亚节)[1,2,3], Mengqi Wang (王梦琦)[1,2,3], Wenyu Yang (杨文宇)[1,2,3], Weixi Chen (陈娓兮)[4], Yejin Zhang (张冶金)[2], and Jiaoqing Pan (潘教青)[1,2,3]

[1] Key Laboratory of Semiconductor Materials Science, Institute of Semiconductors, Chinese Academy of Sciences, Beijing 100083, China

[2] Center of Materials Science and Optoelectronics Engineering, University of Chinese Academy of Sciences, Beijing 100049, China

[3] Beijing Key Laboratory of Low Dimensional Semiconductor Materials and Devices, Beijing 100083, China

[4] School of Physics, Peking University, Beijing 100871, China

*Corresponding author: hyyu09@semi.ac.cn

**Corresponding author: zhouxl@semi.ac.cn

Received March 24, 2020 | Accepted October 19, 2020 | Posted Online February 1, 2021

Gas sensing for measurement of gas components, concentrations, and other parameters plays an important role in many fields. In this Letter, a micro-ring resonator laser used for gas sensing is experimentally demonstrated. The multi-quantum-wells micro-ring laser based on whispering-gallery modes with an annular resonator and an output waveguide was fabricated. A single-mode laser with a wavelength of 1746.4 nm was fabricated for the first time, to the best of our knowledge, experimentally. The output power of 1.65 mW under 40 mA injection current was obtained with a side-mode suppression ratio over 33 dB.

Keywords: gas sensing; whispering-gallery mode; micro-ring resonator laser.

DOI: 10.3788/COL202119.041406

1. Introduction

Accurate measurement of gas components, concentrations, and other parameters plays an important role in many fields. The spectroscopic method, based on the principle of absorption, emission, and scattering of light by gas molecules, with the advantages of non-contact, rapid response, and high selectivity, meeting the requirements of gas measurement under different environmental conditions, is an efficient way for gas sensing[1].

Nowadays, most semiconductor lasers used for gas sensing are distributed feed-back (DFB) lasers and distributed Bragg reflector (DBR) lasers. However, power consumption and volumes of DFB and DBR lasers are hard to reduce any more, which adversely affect cost reduction and device miniaturization. The microcavity laser with low power consumption and small volume was expected to replace them as a suitable light source. Microcavities can be divided into three types, which are the Fabry–Perot (FP) microcavity, photonic crystal (PC) microcavity, and whispering-gallery (WG) microcavity[2]. The FP microcavity is formed by reflection between two reflectors, like the vertical-cavity surface-emitting laser (VCSEL). Generally, to achieve an effective reflectance of over 99%, more than 20 pairs of DBRs are required. However, the FP microcavity laser is surface emitting, which is not conducive to the integration of light sources and other devices[3,4]. The PC microcavity introduces irregular defects in a perfect PC; when the defects are located in the photonic band gap, light waves with wavelengths at this level will be confined to the defect state, so the PC can form a very high-quality (Q) factor local state in a very small area[5,6]. But, the material growth and device fabrication of these two methods are too complex. Thus, the WG microcavity semiconductor laser with considerably low power consumption, small volume, and simple fabrication process can be considered as the light source of the gas sensing system[7]. The WG microcavity has a high-Q factor and small cavity size comparable to an optical wavelength. Light reflected from active area on the wall of the microcavity can provide strong optical confinement, which results in very high cavity Q factors and low thresholds. But, most of the existing WG mode (WGM) microcavity lasers are lasing at 1.3 μm and 1.5 μm, as we know, and lasers emitting from 1700 nm to 2000 nm have not been developed yet. However, lasers emitting at the near infrared (NIR) band from 1700 to 2000 nm contain the absorption region of many gas species like HCl, H_2O, and HBr, which are of great significance for gas sensing[8].

In this Letter, a micro-ring resonator laser used for gas sensing is experimentally demonstrated. The laser consists of a resonator with a 15 μm outer radius, 8 μm inner radius, and output waveguide of 3 μm in width. Single-mode lasing was obtained, for the first time, to the best of our knowledge, at about 1746.4 nm at 288 K. The maximum output power is 1.65 mW with a side-mode suppression ratio (SMSR) over 33 dB.

2. Simulation and Calculation

The simulation of the micro-ring resonator laser was based on the finite element method (FEM), which uses a variation of Maxwell equations as the characteristic equations. For example, the characteristic equation of the transverse electric (TE) mode can be described by[9]

$$\nabla \times (\mu_r^{-1} \nabla \times E) - \left(\varepsilon_r - \frac{i\sigma}{\omega}\varepsilon_0\right) k_0^2 E = 0, \tag{1}$$

where μ_r is the relative permeability, and ε_r is the relative dielectric constant. The frequency and Q factor characteristics of the eigen-mode can be obtained by calculating the characteristic solution of the equation f. The Q factor can be defined as

$$Q = \frac{\mathrm{Real}(f)}{2|\mathrm{Imag}(-f)|}. \tag{2}$$

To forecast the Q factor and mode field distribution of the device, we simulated a micro-ring resonator laser with a 15 μm outer radius, 8 μm inner radius resonator, and a 3 μm wide output waveguide by the two-dimensional (2D) FEM method. The micro-ring resonator and output waveguide with refractive index of 3.2 are confined by air instead of the SiO_2 insulating layer and the p-electrode layer, as in real devices, which has a refractive index of 1.54. Simulation result of the Q value varying with different wavelengths is plotted in Fig. 1(a). A single mode emitting at 1746.3 nm is obtained with a higher-Q factor of 1.42×10^5. Figure 1(b) shows the mode field distribution of 1746.3 nm.

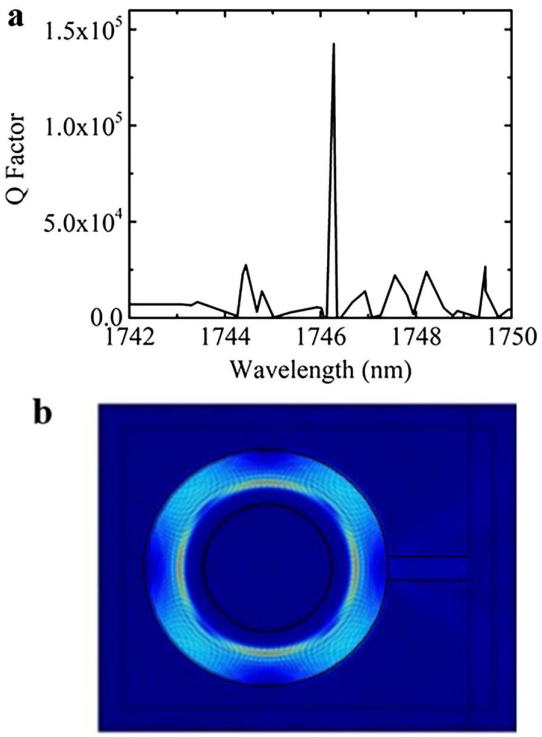

Fig. 1. (a) Simulation result of the quality factor (Q). (b) Electric field distribution.

3. Fabrication

The fabrication process of the micro-ring resonator laser includes materials epitaxy, photolithography, dry etching, wet etching, metal sputtering, etc. All of these processes can be summarized into two steps, which are materials epitaxy and manufacturing process.

Materials of the laser were grown by metal organic chemical vapor deposition (MOCVD) equipment. Table 1 shows the epitaxial structure of the laser. The whole structure was grown on an InP substrate. Referring to the previous research of semiconductor lasers emitting at 1.7–1.8 μm[10–12], and making full use of the mature manufacturing process of InP/InGaAsP materials, we choose InGaAs/InGaAsP as the active region materials of the laser. The In component of InGaAs quantum wells (QWs) with a center wavelength of 1.75 μm takes about 80%. The lattice mismatch of the quantum well material is 1.9%. The optical gain of the QWs structure was calculated with the variations of wavelength and carrier concentration, as shown in Fig. 2. Growth interruption was an effective way to improve the interface Q of QWs, which are influenced by the large lattice mismatch value. In order to confine the carrier and the optical field in the active layers effectively, the upper and lower separated confinement heterostructure (SCH) layers are formed by 120 nm InGaAsP with a band-gap wavelength of 1.3 μm (1.3 Q), respectively. With lower refractive indices, 1700 nm Zn-doped and 750 nm Si-doped InP layers formed the cladding layer and the buffer layer, which were used for reducing defects and limiting

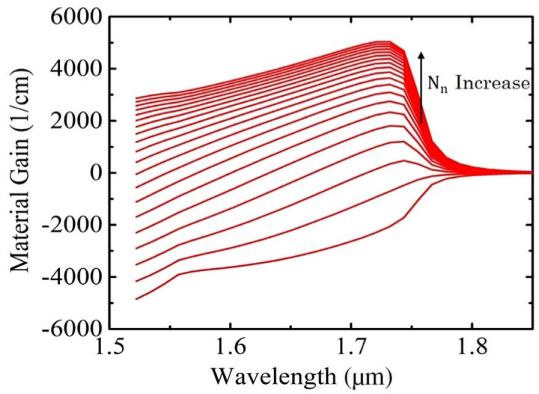

Fig. 2. Optical gain of the QW structure varying with wavelength and carrier concentration N_n.

Table 1. Epitaxial Structure of the Laser.

No.	Item Name	Thickness (nm)	Doping
0	N-InP (Substrate)	/	Si
1	N-InP (Buffer)	750	Si
2	1.3 Q InGaAsP (Lower SCH)	120	/
3	Active area (MQWs)	QW: 9.5 × 4 QB: 12 × 5	/
4	1.3 Q InGaAsP (Upper SCH)	120	/
5	P-InP (Cladding)	1700	Zn
6	P-InGaAs (Contact)	200	Zn

the light field. A 200 nm InGaAs was deposited on the top of the whole structure as a contact layer.

Etching high-Q resonators with a vertical and smooth sidewall plays the core role in the whole production process of the device. Since the wet etching method always has directional selectivity and will lead to a lateral etching, the microcavity was etched by the inductively coupled plasma (ICP) etching method. As a hard mask for etching, 500 nm SiO_2 was deposited by plasma-enhanced chemical-vapor deposition (PECVD) on the InGaAs contact layer. The micro-ring resonator and a short output waveguide pattern were transferred onto the SiO_2 layer using standard photolithography and ICP etching techniques. Under the cover of a SiO_2 mask, the underlying material was etched by ICP as well. To reduce optical absorption losses and ensure lasing Q, the etching depth needs to be about 4.5 μm. The cross-sectional view scanning electron microscope (SEM) image of the etching result is shown in Fig. 3(a). After ICP etching, the next significant production process is electrode preparation. To efficiently pump the WGM region, the electrode contact is just over the resonator. A Ti–Au p electrode layer was formed over the wafer by magnetron sputtering, and the electrode pattern was defined by wet etching. The wafer was thinned down to 150 μm, and an Au–Ge–Ni–Au later was formed as an n-type contact on the back of the InP substrate by metal evaporation. After rapid thermal annealing, the device was completed. Figure 3(b) shows the top-view SEM image of the finished device.

4. Experimental Results and Discussion

The laser was tested on a thermoelectric cooler (TEC), and the temperature was controlled at 288 K. Light power and voltage versus the injection current (PIV) were collected by an integrating sphere, and the PIV curves under 40 mA are plotted in Fig. 4. The light power can come up to about 1.65 mW when the injection current was 40 mA, as shown in Fig. 4. But, the threshold current of the laser cannot be confirmed through these PIV curves. Because of the small laser volume, the spontaneous

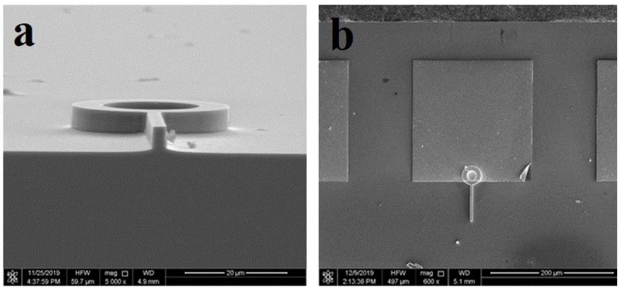

Fig. 3. (a) Cross-sectional view SEM image of the etched ring. (b) Top-view SEM image of the device with a metal electrode, a micro-ring resonator, and an output waveguide.

emission rate is high; almost all of the spontaneous emissions are coupled to the single lasing mode. In addition, due to the high value of the Q factor, most of the spontaneous emission light is confined in the microcavity, resulting in a high intensity. Therefore, the power-current curve does not have an inflection point, so the threshold current cannot be confirmed[13].

The lasing spectra were measured by an optical spectrum analyzer with a resolution of 0.05 nm. Light lasing from the device was partially coupled into a tapered fiber and transmitted to the optical spectrum analyzer through a multimode optical fiber. The lasing spectrum at an injection current of 40 mA is shown in Fig. 5. As the figure shows, the central wavelength is 1746.4 nm with SMSR of 33.33 dB. Obviously, only fundamental transverse mode lasing is achieved because the high-order transverse modes are completely suppressed by the ring resonator. To characterize the stability of the device, the spectra under different inject currents were tested. When the injection current varies from 20 mA to 50 mA, with an interval of 10 mA, the central wavelengths are 1745.18 nm, 1745.73 nm, 1746.37 nm, and 1747.07 nm, with the SMSR of 19.30 dB, 31.93 dB, 33.33 dB, and 25.09 dB, respectively, as shown in Fig. 5. The change is 0.063 nm per milliampere as calculated.

Compared with DFB and DBR lasers[14], whose volumes are hundreds of millimeters and threshold currents are at least tens of milliamps, the volume of our WGM micro-ring resonator

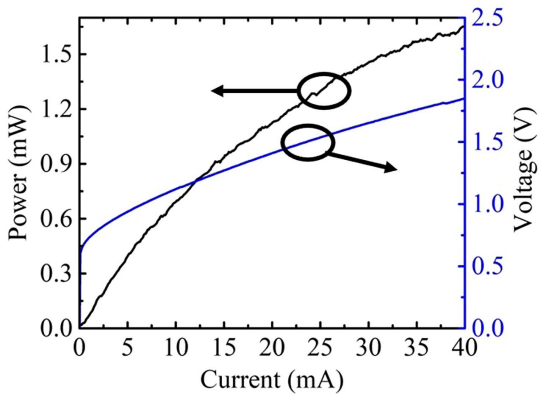

Fig. 4. Output power and applied voltage versus the injection current for a micro-ring resonator laser.

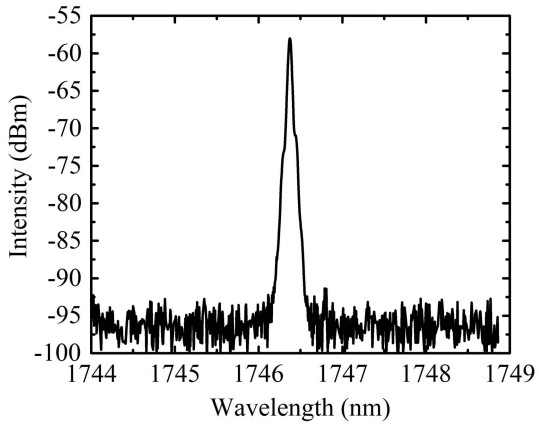

Fig. 5. Lasing spectrogram for the micro-ring resonator laser at an injection current of 40 mA.

laser is much smaller, and the threshold current is lower too. Compared with other WGM micro-resonator lasers[15–19], our device has a higher lasing power. Thus, we think the low-power consumption, small volume laser is competitive and has potential in gas sensing.

5. Conclusion

In conclusion, a WGM micro-ring resonator laser used for gas sensing is experimentally demonstrated. The laser is based on multi-InGaAs/InGaAsP-QWs and an InP substrate. It consists of a resonator with a 15 μm outer radius and 8 μm inner radius, and a 3 μm wide output waveguide. The maximum output power is 1.65 mW at 288 K, as shown in the PIV curve. The lasing spectrum shows that a single-mode lasing was obtained, for the first time, to the best of our knowledge, at about 1746.4 nm at 288 K, with an SMSR over 33 dB.

Compared with other lasers like DFB and DBR lasers, the WG micro-ring resonator laser has a much smaller volume and much lower threshold current, making it promising in gas sensing.

Acknowledgement

This work was supported by the National Key Research and Development Project (Nos. 2017YFB0405300 and 2018YFA0209001), National Natural Science Foundation of China (NSFC) (Nos. 61934007 and 61974141), and Beijing Municipal Science and Technology Project (Nos. Z191100004819011 and 4182064).

References

1. W. Liu, Z. Cui, and F. Dong, "Optical and spectroscopic techniques for environmental pollution monitoring," Optoelectron. Technol. Inf. **15**, 1 (2002).
2. K. J. Vahala, "Optical microcavities," Nature **424**, 839 (2003).
3. K. Liu, Q. Wei, Y. Huang, X. Duan, Q. Wang, X. Ren, and S. Cai, "Integrated optoelectronic chip pair for transmitting and receiving optical signals simultaneously," Chin. Opt. Lett. **17**, 041301 (2019).
4. C. J. Hood, H. J. Kimble, and J. Ye, "Characterization of high-finesse mirrors: loss, phase shifts, and mode structure in an optical cavity," Phys. Rev. A **64**, 033804 (2001).
5. O. Painter, R. K. Lee, A. Scherer, A. Yariv, J. D. O'Brien, P. D. Dapkus, and I. Kim, "Two-dimensional photonic band-gap defect mode laser," Science **284**, 1819 (1999).
6. Q. Yuan, L. Fang, Q. Zhao, Y. Wang, B. Mao, V. Khayrudinov, H. Lipsanen, Z. Sun, J. Zhao, and X. Gan, "Mode couplings of a semiconductor nanowire scanning across a photonic crystal nanocavity," Chin. Opt. Lett. **17**, 062301 (2019).
7. Z. Z. Shen, Y.-Z. Hao, F.-L. Wang, K. Yang, H. Y. Yu, J.-Q. Pan, Y.-D. Yang, J.-L. Xiao, and Y.-Z. Huang, "Hybrid square/rhomb-rectangular semiconductor lasers for ethylene detection," in *Conference on Lasers and Electro-Optics* (2019), paper JW2A.3.
8. W. Zeller, L. Naehle, P. Fuchs, F. Gerschuetz, L. Hildebrandt, and J. Koeth, "DFB lasers between 760 nm and 16 μm for sensing applications," Sensors **10**, 2492 (2010).
9. X. Ma, "Investigations on coupled cavity lasers and optically injected microcavity lasers," PhD Dissertation (Institute of Semiconductors, CAS, 2017).
10. J. Mi, H. Yu, L. Yuan, S. Li, M. Li, S. Liang, Q. Kan, and J. Pan, "Distributed Bragg reflector laser (1.8 μm) with 10 nm wavelength tuning range," Chin. Opt. Lett. **13**, 041401 (2015).
11. B. Niu, H. Yu, L. Yu, D. Zhou, L. Zhao, J. Pan, and W. Wang, "1.65 μm three-section distributed Bragg reflective (DBR) laser for CH_4 gas sensor," J. Semiconduct. **34**, 85550Z (2012).
12. H. Yu, P. Wang, J. Mi, X. Zhou, J. Pan, H. Wang, L. Xie, and W. Wang, "1.8-μm DBR lasers with over 11-nm continous wavelength tuning range for multi-species gas detection," in *2017 Asia Communications and Photonics Conference (ACP)* (2017), p. 1.
13. L. He, Ş. K. Ozdemir, and L. Yang, "Whispering gallery microcavity lasers," Laser Photon. Rev. **7**, 60 (2013).
14. T. R. Chen, P. C. Chen, J. Ungar, J. Paslaski, S. Oh, H. Luong, and N. Bar-Chaim, "Wide temperature range linear DFB lasers with very low threshold current," Electron. Lett. **33**, 963 (1997).
15. Y. Huang, X. Ma, Y. Yang, J. Xiao, and Y. Du, "Hybrid-cavity semiconductor lasers with a whispering-gallery cavity for controlling *Q* factor," Sci. Chin. Inf. Sci. **61**, 080401 (2018).
16. Y. Huang, K. Che, Y. Yang, S. Wang, Y. Du, and Z. Fan, "Directional emission InP/GaInAsP square-resonator microlasers," Opt. Lett. **33**, 2170 (2008).
17. M. Munsch, J. Claudon, N S. Malik, K. Gilbert, P. Grosse, J.-M. Gérard, F. Albers, F. Langer, T. Schlereth, M. M. Pieczarka, S. Höfling, M. Kamp, A. Fochel, and S. Reitzenstein, "Room temperature, continuous wave lasing in microcylinder and microring quantum dot laser diodes," Appl. Phys. Lett. **100**, 031111 (2012).
18. S. Sui, M. Tang, Y. Yang, J. Xiao, Y. Du, and Y. Huang, "Single-mode hybrid AlGaInAs/Si octagonal-ring microlaser with stable output," Chin. Opt. Lett. **14**, 031402 (2016).
19. Y. Yang, S. Sui, M. Tang, J. Xiao, Y. Du, A. W. Poon, and Y. Huang, "Hybrid AlGaInAs/Si Fabry–Pérot lasers with near-total mode confinements," J. Semiconduct. **39**, 084001 (2018).